Successive Bayesian Reconstructor for FAS Channel Estimation

Zijian Zhang*, Jieao Zhu*, Linglong Dai*, *Fellow, IEEE*, and Robert W. Heath Jr.†, *Fellow, IEEE*

*Department of Electronic Engineering, Tsinghua University, Beijing 100084, China
*Beijing National Research Center for Information Science and Technology (BNRist), Beijing 100084, China
†Department of Electrical and Computer Engineering, University of California, San Diego, 9500 Gilman Drive, La Jolla, CA 92093, USA
E-mails: {zhangzj20, zja21}@mails.tsinghua.edu.cn; daill@tsinghua.edu.cn; rwheathjr@ucsd.edu

2024 IEEE Wireless Communications and Networking Conference (WCNC) | 979-8-3503-0358-2/24/$31.00 ©2024 IEEE | DOI: 10.1109/WCNC57260.2024.10571302

***Abstract*—Fluid antenna systems (FASs) can reconfigure their locations freely within a spatially continuous space. To keep favorable antenna positions, the channel state information (CSI) acquisition for FASs is essential. While some techniques have been proposed, most existing FAS channel estimators require several channel assumptions, such as slow variation and angular-domain sparsity. When these assumptions are not reasonable, the model mismatch may lead to unpredictable performance loss. In this paper, we propose the successive Bayesian reconstructor (S-BAR) as a general solution to estimate FAS channels. Unlike model-based estimators, the proposed S-BAR is prior-aided, which builds the experiential kernel for CSI acquisition. Inspired by Bayesian regression, the key idea of S-BAR is to model the FAS channels as a stochastic process, whose uncertainty can be successively eliminated by kernel-based sampling and regression. In this way, the predictive mean of the regressed stochastic process can be viewed as the maximum a posterior (MAP) estimator of FAS channels. Simulation results verify that, in both model-mismatched and model-matched cases, the proposed S-BAR can achieve higher estimation accuracy than the existing schemes.**

I. INTRODUCTION

In recent years, fluid antenna systems (FASs), also called fluid antennas or movable antennas, are proposed to achieve higher diversity and multiplexing gains than conventional multiple-input multiple-output (MIMO) systems [1]–[3]. Different from MIMO with fixed antennas, FAS introduces a structure where a few fluid antennas can freely switch their locations within a given space [4]. In this way, the spacing of the available locations (referred to as "ports") for fluid antennas can be arbitrarily small. This almost continuously movable feature allows FASs to keep fluid antennas at favorable positions, thus promising to achieve high diversity and multiplexing gains with very few antennas [1]–[3].

Despite these encouraging prospects, the expected gains of FASs are hard to achieve in practice. In specific, the transmission performance of FASs heavily relies on the positions of fluid antennas [5]–[7]. To ensure favorable antenna placements, the channel state information (CSI) knowledge of available locations is essential [8]–[10]. However, the channel estimation for FASs is challenging. The reason is that, the allowed locations (i.e., the ports) of fluid antennas are densely deployed, leading to very high-dimensional port channels [4]. Thereby, it requires an unacceptable number of pilots to acquire the channels. Besides, limited by the hardware structure of FASs, only a few ports can be connected to radio frequency (RF) chains for channel measurements within the coherence time, which exacerbates the difficulty of channel estimation. To address the high-dimensional FASs channels, pilot-reduced channel estimators have been investigated in [8]–[10]. However, most existing channel estimators rely on some channel assumptions, such as the slow variation [8], angle-domain sparsity [9], and known angles-of-arrival (AoAs) [10]. When these assumptions are not reasonable, the model mismatch will lead to an unpredictable performance loss.

In this paper, we propose the successive Bayesian reconstructor (S-BAR) as a general solution to estimate FAS channels. Different from the existing model-based estimators relying on channel assumptions, the proposed S-BAR builds the experiential kernel of FASs channels for CSI acquisition. Specifically, inspired by the Bayesian regression [11], the key idea of S-BAR is to model the FAS channels as a stochastic process with an experiential kernel, which characterizes the inherent correlation of FAS channels. Then, the uncertainty of the stochastic process can be successively eliminated by kernel-based sampling and regression. Particularly, the proposed S-BAR is a two-stage scheme. In the first stage, the measured channels are determined by following the principle of maximum posterior variance. In the second stage, the channel measurements are combined with the experiential kernel for process regression. Then, the mean of the regressed stochastic process is exactly the maximum a posterior (MAP) estimator of FAS channels. Simulation results reveal that, in both model-mismatched and model-matched cases, the proposed S-BAR can achieve higher estimation accuracy than the existing schemes based on channel assumptions.

The rest of this paper is organized as follows. In Section II, the system model of an FAS is introduced, and the problem of channel estimation is formulated. In Section III, the general S-BAR is proposed for FAS channel estimation. In Section IV, simulation results are presented to evaluate the estimation performance. Finally, conclusions are drawn in Section V.

Notation: $[\cdot]^{-1}$, $[\cdot]^{*}$, $[\cdot]^{\mathrm{T}}$, and $[\cdot]^{\mathrm{H}}$ denote the inverse, conjugate, transpose, and conjugate-transpose operations, respectively; $\mathbf{x}(i)$ denotes the i-th entry of vector $\mathbf{x}$; $\mathbf{X}(i,j)$, $\mathbf{X}(j,:)$ and $\mathbf{X}(:,j)$ denote the (i,j)-th entry, the j-th row, and the j-th column of matrix $\mathbf{X}$, respectively; $\mathrm{Tr}(\cdot)$ denotes the trace of its argument; $\mathsf{E}(\cdot)$ is the expectation of its argument; $\dim(\cdot)$ is the dimensional of its argument; $\mathcal{CN}(\boldsymbol{\mu},\boldsymbol{\Sigma})$ and $\mathcal{GP}(\boldsymbol{\mu},\boldsymbol{\Sigma})$ respectively denote the complex Gaussian distribution and complex Gaussian process, with mean $\boldsymbol{\mu}$ and covariance $\boldsymbol{\Sigma}$; $\mathbf{0}_L$ is an all-zero vector or matrix with dimension L.

979-8-3503-0358-2/24/$31.00 ©2024 IEEE

II. System Model

In this paper, we consider the narrowband channel estimation in an uplink FAS, which consists of an N-port base station (BS) equipped with M fluid antennas and a single-antenna user. The N feeding ports are uniformly distributed along a linear dimension at the receiver. The M fluid antennas can be repositioned to the M locations of N available ports ($M \ll N$), and each antenna is connected to an RF chain. Let $\mathbf{h} \in \mathbb{C}^N$ denote the channels of N ports, and let P denote the number of transmit pilots within a coherence time frame. To characterize the locations of M fluid antennas in timeslot p, we introduce the definition of switch matrix as follows:

Definition 1 (Switch Matrix): Binary indicator $\mathbf{S}_p \in \{0,1\}^{M\times N}$ is defined as the switch matrix of multiple fluid antennas in timeslot p. The (m,n)-th entry being 1 (or 0) means that the m-th antenna is (or not) located at the n-th port. Since M of N ports are selected in each timeslot, each row of $\mathbf{S}_p$ has one entry of 1, and all entries of 1 in $\mathbf{S}_p$ are not in the same column, i.e., $\|\mathbf{S}_p(m,:)\| = 1$ for all $m \in \{1,\cdots,M\}$, $\|\mathbf{S}_p(:,n)\| \in \{0,1\}$ for all $n \in \{1,\cdots,N\}$, and $\mathbf{S}_p\mathbf{S}_p^{\mathrm{H}} = \mathbf{I}_M$.

Utilizing **Definition 1**, the signal vector $\mathbf{y}_p \in \mathbb{C}^M$ received at the BS in timeslot p can be modeled as

$$\mathbf{y}_p = \mathbf{S}_p\mathbf{h}s_p + \mathbf{z}_p, \tag{1}$$

where s_p is the pilot transmitted by the user and $\mathbf{z}_p \sim \mathcal{CN}\left(\mathbf{0}_M, \sigma^2\mathbf{I}_M\right)$ is the additive white Gaussian noise (AWGN) at M selected ports. Without loss of generality, we assume that $s_p = 1$ for all $p \in \{1,\cdots,P\}$. Considering the total P timeslots for pilot transmission, we arrive at

$$\mathbf{y} = \mathbf{S}\mathbf{h} + \mathbf{z}, \tag{2}$$

where $\mathbf{y} := \left[\mathbf{y}_1^{\mathrm{T}},\cdots,\mathbf{y}_P^{\mathrm{T}}\right]^{\mathrm{T}}$, $\mathbf{S} := \left[\mathbf{S}_1^{\mathrm{T}},\cdots,\mathbf{S}_P^{\mathrm{T}}\right]^{\mathrm{T}}$, and $\mathbf{z} := \left[\mathbf{z}_1^{\mathrm{T}},\cdots,\mathbf{z}_P^{\mathrm{T}}\right]^{\mathrm{T}}$. Our goal is to reconstruct the N-dimensional channel $\mathbf{h}$ according to the PM-dimensional noisy pilot $\mathbf{y}$. Since fluid antennas move almost continuously, N is much larger than PM ($N \gg PM$). Besides, due to the zero-one distribution of $\mathbf{S}$, most elements of $\mathbf{h}$ cannot be observed directly or indirectly. As a result, the channel estimation of FASs is usually challenging.

III. Proposed Successive Bayesian Reconstructor

In this section, based on the Bayesian regression, we propose the S-BAR as a general solution to realize FAS channel estimation. Specifically, in Subsection III-A, the classical Bayesian regression is introduced. Then, in Subsection III-B, the proposed S-BAR scheme is illustrated. Finally, in Subsection III-C, the kernel selection of S-BAR is discussed.

A. Bayesian Regression

Without making any prior assumptions, the attempt to recover the function $f(\mathbf{x})$ from a few samples appears to be a challenging endeavor. Fortunately, by building the experiential kernel of $f(\mathbf{x})$, Bayesian regression can determine the sampling strategy and reconstruct $f(\mathbf{x})$ with a few samples in a non-parametric way. Under this framework, Gaussian process regression (GPR) has become a popular solution [11]. Specifically, function $f(\mathbf{x})$ can be modeled as a sample of Gaussian process $\mathcal{GP}\left(\mu\left(\mathbf{x}\right), k\left(\mathbf{x},\mathbf{x}'\right)\right)$. It is completely specified by its mean $\mu\left(\mathbf{x}\right)$ and its kernel $k\left(\mathbf{x},\mathbf{x}'\right)$, which encodes the smoothness of regressed $f(\mathbf{x})$. In timeslot t, consider a prior $\mathcal{GP}\left(\mu\left(\mathbf{x}\right), k\left(\mathbf{x},\mathbf{x}'\right)\right)$ over $f(\mathbf{x})$. Let $\boldsymbol{\gamma}^t := [\gamma^1,\cdots,\gamma^t]^{\mathrm{T}}$ denote t noisy measurements for points in $\mathcal{A}^t := \{\mathbf{x}^1,\cdots,\mathbf{x}^t\}$, where $\gamma^i = f(\mathbf{x}^i) + n_i$ with $n_i \sim \mathcal{CN}\left(0,\delta^2\right)$. It is easy to prove that, given $\boldsymbol{\gamma}^t$, the posterior over $f(\mathbf{x})$ is also a Gaussian process whose mean and covariance are

$$\mu^t\left(\mathbf{x}\right) = \mu\left(\mathbf{x}\right) + \left(\mathbf{k}^t(\mathbf{x})\right)^{\mathrm{H}}\left(\mathbf{K}^t + \delta^2\mathbf{I}_t\right)^{-1}\left(\boldsymbol{\gamma} - \boldsymbol{\mu}^t\right), \tag{3}$$

$$k^t\left(\mathbf{x},\mathbf{x}'\right) = k\left(\mathbf{x},\mathbf{x}'\right) - \left(\mathbf{k}^t(\mathbf{x})\right)^{\mathrm{H}}\left(\mathbf{K}^t + \delta^2\mathbf{I}_t\right)^{-1}\mathbf{k}^t(\mathbf{x}'), \tag{4}$$

where $\mathbf{k}^t(\mathbf{x}) := \left[k\left(\mathbf{x}^1,\mathbf{x}\right),\cdots,k\left(\mathbf{x}^t,\mathbf{x}\right)\right]^{\mathrm{T}}$; $\boldsymbol{\mu}^t := \left[\mu\left(\mathbf{x}^1\right),\cdots,\mu\left(\mathbf{x}^t\right)\right]^{\mathrm{T}}$; and the (i,j)-th entry of $\mathbf{K}^t \in \mathbb{C}^{t\times t}$ is $k\left(\mathbf{x}^i,\mathbf{x}^j\right)$, for all $i,j \in \{1,\cdots,t\}$.

Then, the next candidate point to be sampled, i.e., $\mathbf{x}^{t+1}$, can be determined based on the updated posterior. For successive sampling, sampling the point with the maximum posterior variance can obtain the most information. By assuming that $\mathbf{x} \in \mathcal{S}$, $\mathbf{x}^{t+1}$ can be chosen according to

$$\mathbf{x}^{t+1} = \underset{\mathbf{x}\in\mathcal{S}/\mathcal{A}^t}{\arg\max}\ k^t\left(\mathbf{x},\mathbf{x}\right), \tag{5}$$

where $/$ is the set difference. By letting $t \to \infty$, the value of variance $k^t\left(\mathbf{x},\mathbf{x}\right)$ decreases asymptotically, which means that the uncertainty of $f(\mathbf{x})$ is reduced. After reaching the tolerance threshold, the posterior mean $\mu^t\left(\mathbf{x}\right)$ can be viewed as a MAP estimator of $f(\mathbf{x})$ [11].

B. Proposed S-BAR Scheme

In each pilot timeslot, M fluid antennas move positions and measure channels, thus the channel estimation of FASs is similar to a successive sampling process. Since the port spacing is short, the FAS channels are highly correlated. These features inspire us to recover $\mathbf{h}$ through Bayesian regression. To reconstruct FAS channels based on experiential kernel, we model $\mathbf{h}$ as a sample of Gaussian process $\mathcal{GP}\left(\mathbf{0}_N, \boldsymbol{\Sigma}\right)$. Semidefinite Hermitian matrix $\boldsymbol{\Sigma} \in \mathbb{C}^{N\times N}$ is called the kernel or prior covariance, of which the selection will be introduced in Subsection III-C. Then, the proposed S-BAR scheme is summarized in **Algorithm 1**. For clarity, the basic principle of S-BAR is firstly introduced as follows.

1) Algorithmic Principle: At some moment, let Ω denote the index sequence of the measured channels and let $\mathbf{y}_\Omega \in \mathbb{C}^{\dim(\Omega)}$ denote the corresponding received pilots, which is from $\mathbf{y}_\Omega = \mathbf{h}\left(\Omega\right) + \mathbf{z}_\Omega$ with $\mathbf{z}_\Omega \sim \mathcal{CN}(\mathbf{0}_{\dim(\Omega)}, \sigma^2\mathbf{I}_{\dim(\Omega)})$ being the AWGN. For given $\mathbf{y}_\Omega$, the posterior mean $\boldsymbol{\mu}_\Omega$ and posterior covariance $\boldsymbol{\Sigma}_\Omega$ of $\mathbf{h}$ can be calculated by:

$$\boldsymbol{\mu}_\Omega = \boldsymbol{\Sigma}(:,\Omega)\left(\boldsymbol{\Sigma}(\Omega,\Omega) + \sigma^2\mathbf{I}_{\dim(\Omega)}\right)^{-1}\mathbf{y}_\Omega, \tag{6}$$

$$\boldsymbol{\Sigma}_\Omega = \boldsymbol{\Sigma} - \left(\boldsymbol{\Sigma}(\Omega,:)\right)^{\mathrm{H}}\left(\boldsymbol{\Sigma}(\Omega,\Omega) + \sigma^2\mathbf{I}_{\dim(\Omega)}\right)^{-1}\boldsymbol{\Sigma}(\Omega,:). \tag{7}$$

For given Ω, the next candidate channel to be measured can be determined by finding the index associated with the largest posterior variance, i.e.,

$$n^\star = \underset{n\in\{1,\cdots,N\}/\Omega}{\arg\max}\ \boldsymbol{\Sigma}_\Omega(n,n). \tag{8}$$

Algorithm 1 Proposed Successive Bayesian Reconstructor

Input: Number of pilots P, kernel $\mathbf{\Sigma}$.
Output: Reconstructed FAS channel $\hat{\mathbf{h}}$.

```
# Stage 1 (Offline Design):
Initialization: Ω = ∅, S_p = 0_{M×N} for all p ∈ {1, ···, P}
for p ∈ {1, ···, P} do
    for m ∈ {1, ···, M} do
        Posterior covariance update: Calculate Σ_Ω by (7)
        Candidate selection: n* = argmax_{n∈{1,···,N}/Ω} Σ_Ω(n, n)
        Switch matrix update: S_p(m, n*) = 1
        Sequence update: Ω = Ω ∪ {n*}
    end for
end for
Merge switch matrices: S := [S_1^T, ···, S_P^T]^T
Weight calculation: w = (Σ(Ω, Ω) + σ^2 I_{PM})^{-1} Σ(Ω, :)
# Stage 2 (Online Regression):
Employ the designed switch matrix S at the BS, and then
    obtain the received pilot: y = Sh + z
Channel reconstruction: ĥ = w^H y
return Reconstructed FAS channel ĥ
```

Subsequently, we can update Ω by $\Omega \cup \{n^\star\}$ and repeat the above process until the posterior mean $\boldsymbol{\mu}_\Omega$ can well approximate $\mathbf{h}$.

2) Observations: From the above equations, we obtain the following three observations.

- (6) indicates that, the posterior mean $\boldsymbol{\mu}_\Omega$ is the linear weighted sum of pilot $\mathbf{y}_\Omega$, i.e., $\boldsymbol{\mu}_\Omega = \mathbf{w}^{\mathrm{H}}\mathbf{y}_\Omega$, wherein the weight $\mathbf{w} := \left(\mathbf{\Sigma}(\Omega,\Omega) + \sigma^2\mathbf{I}_{\dim(\Omega)}\right)^{-1}\mathbf{\Sigma}(\Omega,:)$ only relies on the kernel $\mathbf{\Sigma}$.
- (7) shows that posterior covariance $\mathbf{\Sigma}_\Omega$ only relies on kernel $\mathbf{\Sigma}$ and is unrelated to the received pilot $\mathbf{y}_\Omega$.
- (8) suggests that the next channel to be measured only relies on the posterior covariance $\mathbf{\Sigma}_\Omega$.

These observations reveal that, the switch matrix $\mathbf{S}$ and the weight $\mathbf{w}$ are unrelated to the received pilot $\mathbf{y}$, thus they can be designed offline and then deployed online to reduce the complexity. Thereby, the proposed S-BAR can be realized in the following two stages.

3) Stage 1 (Offline Design): Since index sequence Ω is determined by the posterior covariance $\mathbf{\Sigma}_\Omega$, and $\mathbf{\Sigma}_\Omega$ only relies on the kernel $\mathbf{\Sigma}$. The switch matrix $\mathbf{S} \in \{0,1\}^{PM \times N}$ and the weight $\mathbf{w} \in \mathbb{C}^{PM}$ for recovering $\mathbf{h} \in \mathbb{C}^N$ can be designed offline at the first stage. By updating $\mathbf{\Sigma}_\Omega$ in (7) and $n^\star$ in (8) alternatingly until $\dim(\Omega) = PM$, sequence Ω can collect all required indexes of the M selected ports in P pilot timeslots.

Then, recall that we have $\mathbf{h}(\Omega) = \mathbf{S}\mathbf{h}$. To achieve the conversion from Ω to $\mathbf{S}$, we can initialize $\mathbf{S}$ as an all-zero matrix and then fill in an one at the position associated with the selected index in each of its row. Note that, this operation naturally satisfies $\|\mathbf{S}(m,:)\| = 1$ for all $m \in \{1,\cdots,M\}$, $\|\mathbf{S}(:,n)\| \in \{0,1\}$ for all $n \in \{1,\cdots,N\}$, and $\mathbf{S}\mathbf{S}^{\mathrm{H}} = \mathbf{I}_{PM}$. These properties ensure that the designed $\mathbf{S}$ is practically implementable in FASs. After obtaining Ω, the weight for reconstructing $\mathbf{h}$ can be obtained by

$$\mathbf{w} = \left(\mathbf{\Sigma}(\Omega,\Omega) + \sigma^2\mathbf{I}_{PM}\right)^{-1}\mathbf{\Sigma}(\Omega,:). \tag{9}$$

4) Stage 2 (Online Regression): Since *Stage 1* is realized offline, the switch matrix $\mathbf{S}$ and weight $\mathbf{w}$ can be designed and saved at the BS in advance. In *Stage 2*, the scheme is then employed online for channel measurements. The M fluid antennas of the BS will move and receive pilots according to the designed $\mathbf{S}$, arriving at the noisy pilot $\mathbf{y}$. Finally, according to the MAP estimator in (6), channel $\mathbf{h}$ can be reconstructed by $\hat{\mathbf{h}} = \mathbf{w}^{\mathrm{H}}\mathbf{y}$, which completes the proposed S-BAR.

5) Computational Complexity: The proposed S-BAR incorporates a hybrid offline and online implementation process, thereby substantially reducing its computational complexity in practical applications. Specifically, the signal processing of S-BAR is composed of two stages. In *Stage 1*, the computational complexity is dominated by the calculation of posterior covariance $\mathbf{\Sigma}_\Omega$, which is updated PM times. According to (7), the complexity of *Stage 1* is $\mathcal{O}\left(P^2M^2\left(P^2M^2 + NPM + N^2\right)\right)$. In *Stage 2*, the computational complexity is from the weighted sum of received pilot $\mathbf{y}$, i.e., $\hat{\mathbf{h}} = \mathbf{w}^{\mathrm{H}}\mathbf{y}$, thus the computational complexity is $\mathcal{O}(N)$. Note that, although the complexity of *Stage 1* is high, *Stage 1* can be implemented offline in advance. From the perspective of practical employment, the effective complexity of S-BAR scheme is only linear to the number of ports N.

C. Kernel Selection for S-BAR Scheme

The selection of kernel $\mathbf{\Sigma}$ determines the shape and flexibility of the proposed S-BAR, which in turn affects its ability to capture patterns and make accurate reconstruction. Considering the localized correlation property of FAS channels, an appropriate kernel should assign higher similarity to nearby ports and decrease influence rapidly with distance. Let $\mathbf{x}_n$ denote the position of the n-th port. Three kernel selections are recommended as follows.

1) Exponential Kernel: The exponential kernel $\mathbf{\Sigma}_{\exp}$ is a popular choice in regression, given by

$$\mathbf{\Sigma}_{\exp}(n,n') = \alpha^2 e^{-\frac{\|\mathbf{x}_n - \mathbf{x}_{n'}\|^2}{\eta^2}} \tag{10}$$

for all $n, n' \in \{1,\cdots,N\}$, where α and η are adjustable hyperparameters. Compared with the other kernels, the exponential kernel is less sensitive to outliers, which makes it suitable to recover channels without obvious regularity.

2) Bessel Kernel: The Bessel kernel $\mathbf{\Sigma}_{\mathrm{bes}}$ is well-suited for capturing and modeling complex-valued data with oscillatory or periodic patterns, given by

$$\mathbf{\Sigma}_{\mathrm{bes}}(n,n') = \alpha^2 J_v\left(\frac{\|\mathbf{x}_n - \mathbf{x}_{n'}\|}{\eta^2}\right) \tag{11}$$

for all $n, n' \in \{1,\cdots,N\}$, wherein J_v is the v-order Bessel function of the first kind. It has the flexibility to adapt to data that exhibits regular and repeating fluctuations, thus $\mathbf{\Sigma}_{\mathrm{bes}}$ is suitable to reconstruct the channels with periodic patterns.

3) Covariance Kernel: An ideal approach is to use the real covariance of $\mathbf{h}$ as the kernel for reconstruction, i.e., $\mathbf{\Sigma}_{\mathrm{cov}} =$

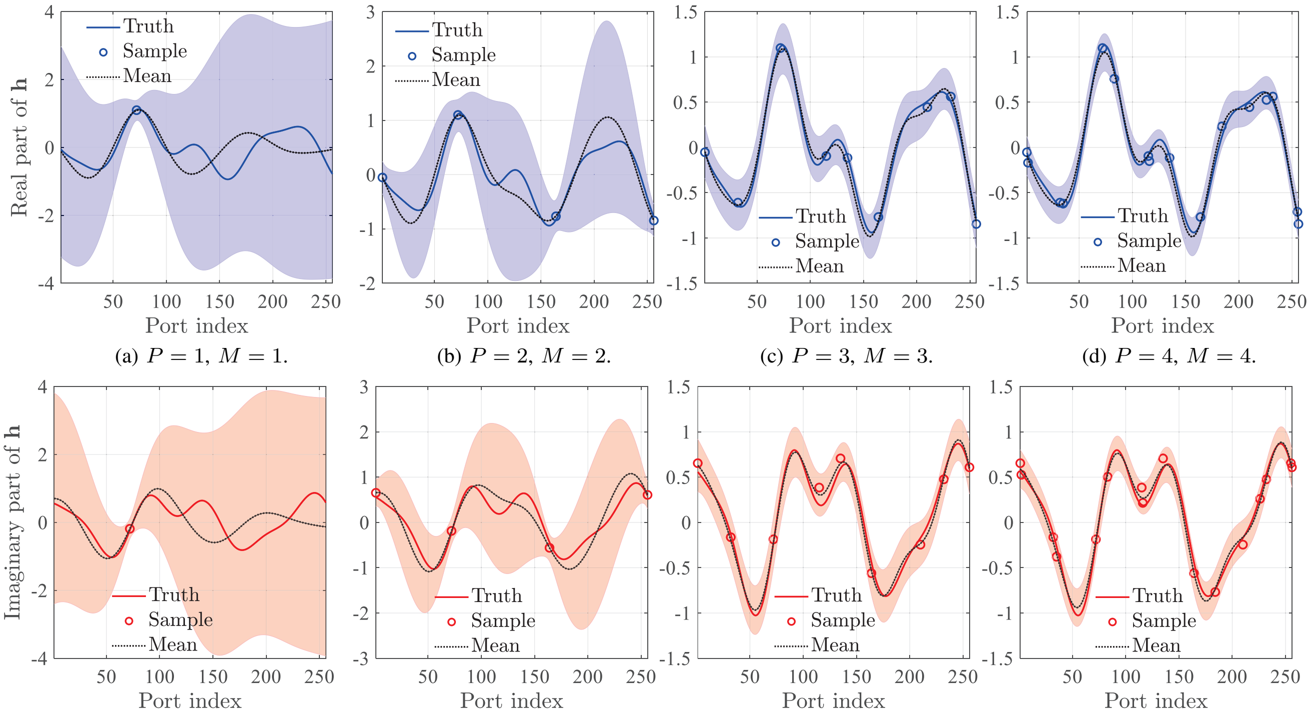

(a) $P = 1$, $M = 1$. (b) $P = 2$, $M = 2$. (c) $P = 3$, $M = 3$. (d) $P = 4$, $M = 4$.

(e) $P = 1$, $M = 1$. (f) $P = 2$, $M = 2$. (g) $P = 3$, $M = 3$. (h) $P = 4$, $M = 4$.

Fig. 1. An illustration of employing S-BAR scheme to estimate FAS channel $\mathbf{h}$. (a)-(d) provide the real part of $\mathbf{h}$ versus the index of ports. (e)-(h) provide the imaginary part of $\mathbf{h}$ versus the index of ports. Particularly, the curve "Truth" denotes the real channel $\mathbf{h}$, and the circle marks denote the sampled (measured) channels. The dotted line "Mean" denotes the posterior mean of Bayesian regression $\boldsymbol{\mu}_\Omega$, i.e., the estimated channel $\hat{\mathbf{h}}$. The highlighted shadows in the figures represent the confidence intervals of $\mathbf{h}$, defined as $[\boldsymbol{\mu}_\Omega(n) - 3\boldsymbol{\Sigma}_\Omega(n,n), \boldsymbol{\mu}_\Omega(n) + 3\boldsymbol{\Sigma}_\Omega(n,n)]$ for the n-th port.

$\mathsf{E}\left(\mathbf{h}\mathbf{h}^{\mathrm{H}}\right)$. Since $\boldsymbol{\Sigma}_{\mathrm{cov}}$ is unknown in practice, we can train an approximated $\boldsymbol{\Sigma}_{\mathrm{cov}}$ before employing S-BAR, given by

$$\boldsymbol{\Sigma}_{\mathrm{cov}} \approx \frac{1}{T}\sum_{t=1}^{T}\mathbf{h}_t\mathbf{h}_t^{\mathrm{H}}, \tag{12}$$

where $\mathbf{h}_t$ is the channel at the t-th training timeslot and T is the number of training timeslots. Since the channel covariance $\mathsf{E}\left(\mathbf{h}\mathbf{h}^{\mathrm{H}}\right)$ does not change so frequently as channels, $\boldsymbol{\Sigma}_{\mathrm{cov}}$ is only updated in a large timescale.

IV. Simulation Results

In this section, simulation results are provided to verify the effectiveness of the proposed S-BAR scheme. Since we have assumed the normalized transmit power, the receiver signal-to-noise ratio (SNR) is defined as $\mathrm{SNR} = \frac{\mathsf{E}\left(\|\mathbf{h}\|^2\right)}{\sigma^2}$, of which the default value is set to 20 dB. Let $\hat{\mathbf{h}}$ denote the estimated value of channel $\mathbf{h}$. The performance is evaluated by the normalized mean square error (NMSE), i.e., $\mathrm{NMSE} = \mathsf{E}\left(\frac{\|\mathbf{h}-\hat{\mathbf{h}}\|^2}{\|\mathbf{h}\|^2}\right)$.

1) Simulation Setup: The simulations are provided based on both the QuaDRiGa channel model and the spatially-sparse clustered (SSC) channel model. For existing model-based estimators, these two models can be viewed as the matched case and mismatched case, respectively. Otherwise particularly specified, the system parameters are set as: $N = 256$, $M = 4$, $P = 10$. The carrier frequency is set to $f_c = 3.5$ GHz, and the length of the fluid antenna array is set to $W = 10\lambda$. For the QuaDRiGa channel model, all parameters are generated according to Table 7.7.1-2 in 3GPP TR 38.901. For the SSC channel model, the number of clusters is set to $C = 9$ and that of rays is set to $R = 100$. Both models have assumed the maximum angle spread to be 5°. For kernel settings, the hyperparameters are set as $\alpha^2 = 1$ and $\eta^2 = \frac{\lambda}{2\pi}$ to generate the exponential kernel $\boldsymbol{\Sigma}_{\mathrm{exp}}$ and Bessel kernel $\boldsymbol{\Sigma}_{\mathrm{bes}}$ [11]. Inspired by the covariance model in [1], [2], the order of Bessel function in $\boldsymbol{\Sigma}_{\mathrm{bes}}$ is set to $\nu = 0$. To account for an ideal baseline, the number of training timeslots is set to $T = 100$ to train the covariance kernel $\boldsymbol{\Sigma}_{\mathrm{cov}}$.

2) Simulation Schemes: We consider the following three schemes for simulations. **1) FAS-OMP:** Assuming that the FAS channels are spatially sparse, the scheme in [9] is modified and employed at the BS to explicitly estimate $\mathbf{h}$. **2) SeLMMSE:** The SeLMMSE proposed in [8] is adopted to estimate channel $\mathbf{h}$, which can be achieved by sequentially measuring channels of PM equally-spaced ports and then using zero-order interpolation to reconstruct $\mathbf{h}$. **3) Proposed S-BAR:** Given a kernel $\boldsymbol{\Sigma}$, the proposed S-BAR scheme, i.e., **Algorithm 1**, is employed to estimate $\mathbf{h}$. Particularly, due to the lack of obvious regularity, the exponential kernel $\boldsymbol{\Sigma}_{\mathrm{exp}}$ is selected as the input of S-BAR for QuaDRiGa channels. Due to their periodic patterns in the spatial domain, the Bessel kernel $\boldsymbol{\Sigma}_{\mathrm{bes}}$ is selected as the input of S-BAR for SSC channels. To provide an ideal baseline, the pre-trained covariance kernel $\boldsymbol{\Sigma}_{\mathrm{cov}}$ is considered for both channel models.

3) Simulation Results: To better understand the working principle of the proposed S-BAR, we plot Fig. 1 to intuitively show its behavior, where the QuaDRiGa channel model is

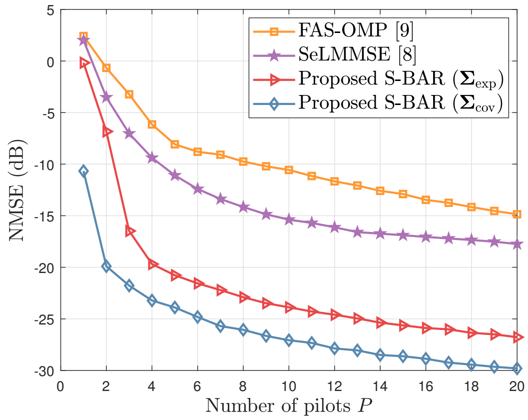

Fig. 2. Model-mismatched case: The NMSE as a function of the number of pilots P under the assumption of QuaDRiGa channel model.

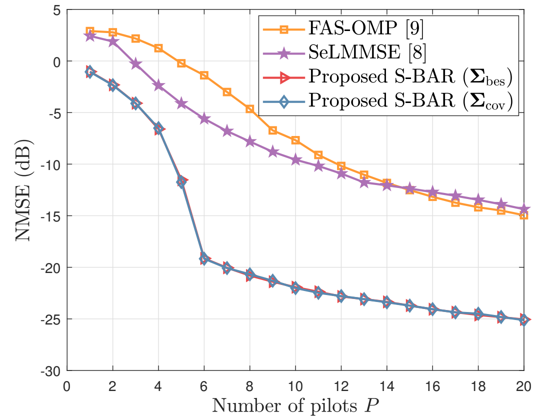

Fig. 3. Model-matched case: The NMSE as a function of the number of pilots P under the assumption of SSC channel model.

considered and the covariance kernel $\mathbf{\Sigma}_{\mathrm{cov}}$ is used to enable S-BAR. From this figure, we have two observations. Firstly, as the number of samples increases, the confidence interval is gradually reduced. It indicates that more pilots or antennas can better eliminate the uncertainty of FAS channels. Secondly, one can note that the sample spacing is usually large. The reason is that, for each sampling, the proposed S-BAR samples the channel with the largest posterior variance. When a port is selected and measured, the channel uncertainty of its nearby ports will decrease, which reduces the trend of selecting them as samples.

Then, we plot the NMSE as a function of the number of pilots P in Fig. 2 for QuaDRiGa model and Fig. 3 for SSC model, respectively. From these two figures, we have the following observations. Firstly, the proposed S-BAR achieves the highest estimation accuracy in both cases. The reason is that, the existing methods do not fully utilize the channel prior for estimation. For FAS-OMP, due to the non-ideal port selection, the information provided by the randomly measured channels may not be sufficient to capture all channel patterns. For SeLMMSE, the unmeasured channels are directly obtained by zero-order interpolation, while their potential estimation errors are not considered. In contrast, the proposed S-BAR incorporates the effect of prior correlation into its estimator, which naturally considers the potential estimation errors of all channels. Through kernel-based sampling and regression, S-BAR can eliminate the uncertainty of many channels with a few pilots. Secondly, the S-BAR enabled by the experiential kernels $\mathbf{\Sigma}_{\mathrm{exp}}$ and $\mathbf{\Sigma}_{\mathrm{bes}}$ can achieve similar performance as that enabled by covariance kernel $\mathbf{\Sigma}_{\mathrm{cov}}$. Recall that $\mathbf{\Sigma}_{\mathrm{exp}}$ and $\mathbf{\Sigma}_{\mathrm{bes}}$ are generated by experiential parameters, while $\mathbf{\Sigma}_{\mathrm{cov}}$ is trained from real channel data. This observation indicates that, even if the real channel covariance $\mathsf{E}\left(\mathbf{h}\mathbf{h}^{\mathrm{H}}\right)$ is unknown, experiential parameters still allow S-BAR to achieve considerable performance.

V. Conclusions

In this paper, we have proposed S-BAR as a general solution to estimate channels in FASs. Different from the existing channel estimators relying on channel assumptions, the general S-BAR utilizes the experiential kernel to acquire CSI in a non-parametric way. Inspired by the Bayesian regression, the proposed S-BAR can select a few informative channels for measurement and combine them with experiential kernel to reconstruct high-dimensional FAS channels. Simulation results reveal that, in both model-mismatched and model-matched cases, the proposed S-BAR can achieve much higher estimation accuracy than the existing schemes.

Acknowledgment

This work was supported in part by the National Natural Science Foundation of China (Grant No. 62031019).

References

[1] K.-K. Wong, A. Shojaeifard, K.-F. Tong, and Y. Zhang, “Fluid antenna systems,” *IEEE Trans. Wireless Commun.*, vol. 20, no. 3, pp. 1950–1962, Mar. 2020.

[2] K.-K. Wong and K.-F. Tong, “Fluid antenna multiple access,” *IEEE Trans. Wireless Commun.*, vol. 21, no. 7, pp. 4801–4815, Jul. 2021.

[3] W. Ma, L. Zhu, and R. Zhang, “MIMO capacity characterization for movable antenna systems,” *IEEE Trans. Wireless Commun. (early access)*, Sep. 2023.

[4] L. Zhu, W. Ma, and R. Zhang, “Movable antennas for wireless communication: Opportunities and challenges,” *arXiv preprint arXiv:2306.02331*, Jun. 2023.

[5] Z. Chai, K.-K. Wong, K.-F. Tong, Y. Chen, and Y. Zhang, “Port selection for fluid antenna systems,” *IEEE Commun. Lett.*, vol. 26, no. 5, pp. 1180–1184, May 2022.

[6] K.-K. Wong, K.-F. Tong, Y. Chen, and Y. Zhang, “Fast fluid antenna multiple access enabling massive connectivity,” *IEEE Commun. Lett.*, vol. 27, no. 2, pp. 711–715, Feb. 2022.

[7] N. Waqar, K.-K. Wong, K.-F. Tong, A. Sharples, and Y. Zhang, “Deep learning enabled slow fluid antenna multiple access,” *IEEE Commun. Lett.*, vol. 27, no. 3, pp. 861–865, Mar. 2023.

[8] C. Skouroumounis and I. Krikidis, “Fluid antenna with linear MMSE channel estimation for large-scale cellular networks,” *IEEE Trans. Commun.*, vol. 71, no. 2, pp. 1112–1125, Feb. 2023.

[9] W. Ma, L. Zhu, and R. Zhang, “Compressed sensing based channel estimation for movable antenna communications,” *arXiv preprint arXiv:2306.04333*, Jun. 2023.

[10] R. Wang, Y. Chen, Y. Hou, K.-K. Wong, and X. Tao, “Estimation of channel parameters for port selection in millimeter-wave fluid antenna systems,” in *Proc. IEEE/CIC Int. Conf. Commun. China (IEEE/CIC ICCC Workshops’23)*, Aug. 2023, pp. 1–6.

[11] C. Williams and C. Rasmussen, “Gaussian processes for regression,” in *Advances in Neural Information Processing Systems*, vol. 8. MIT Press, 1995.